Наносистеми, наноматеріали, нанотехнології
Nanosistemi, Nanomateriali, Nanotehnologii
2021, т. 19, № 2, сс. 281–286

PACS numbers: 61.05.cf, 64.70.Nd, 68.47.Gh, 81.05.Rm, 81.16.Pr, 81.20.Fw, 82.45.Yz

Template Synthesis, Structure, Morphology and Electrochemical Properties of Mesoporous Titania

I. F. Myronyuk[1], V. O. Kotsyubynsky[1], V. L. Chelyadyn[2], V. M. Boychuk[1], and M. A. Hodlevskyi[1]

[1]*Vasyl Stefanyk Precarpathian National University, 57, Shevchenko Str., UA-76018 Ivano-Frankivsk, Ukraine*
[2]*G. V. Kurdyumov Institute for Metal Physics, N.A.S. of Ukraine, 36 Acad. Vernadsky Blvd., UA-03142 Kyiv, Ukraine*

Structure and pore characteristics of the ultrafine titania synthesized from $Ti(OC_4H_9)_4$ in acid medium with cetyltrimethylammonium (CTMA) as template are studied. As determined, the specific surface area and mesopores' volume depend on the pH of reaction medium at the stage of titanium butoxide hydrolysis. The regularities of Li^+-ions' electrochemical intercalation in mesoporous titania with different morphologies are investigated.

Вивчаються характеристики структури та пор ультратонкої титанії, синтезованої з $Ti(OC_4H_9)_4$ у кислотному середовищі з цетилтріметиламмонійом (CTMA) в якості шаблону. Як визначено, питома площа поверхні й об'єм мезопор залежать від pH реакційного середовища на стадії гідролізи бутоксиду титану. Досліджено закономірності електрохемічної інтеркаляції йонів Li^+ у мезопористій титанії з різними морфологіями.

Key words: mesoporous titania, sol–gel route, pore size distribution, anatase phase.

Ключові слова: мезопористий діоксид Титану, золь–ґель-спосіб, розподіл розмірів пор, фаза анатазу.

(Received 7 July, 2020)

1. INTRODUCTION

Nanostructured titania (TiO_2) is one of the most wide used oxide nanomaterial due to its various applications in industry and medi-

cine as a microbiocide, active material for gas sensors and photocatalytic systems, electrode material of dye-sensitized solar cells and electrochemical power sources. Functional characteristics of the titania depend on its phase composition, structural and electronic properties. Particle size and morphology are also important factors, which determine the electric and catalytic parameters of nanodispersed titania. At the same time, synthesis of homogeneous porous materials is an actual. The properties of TiO_2 and its possibility of successful technological application crucially depend on the synthesis method. The sol–gel synthesis of titania involves the chemical conversion of titanium alkoxides, titanyl compounds or titanium tetrachloride into a colloidal product in the liquid-phase reaction medium. The nucleation of specific titanium-dioxide polymorph is caused mostly by the spatial arrangement of the primary monomers $[Ti(OH)_h(OH_2)_{6-h}]^{(4-h)+}$ formed at the hydrolysis and is determined by the pH of reaction medium [1].

2. EXPERIMENTAL DETAILS

Titanium butoxide $Ti(OC_4H_9)_4$ was used as a precursor for titania obtaining; sulphate acid (5M aqueous solution) was used as a hydrolysis agent, and cetyltrimethylammonium chloride (CTMA-Cl) was a template. The hydrolysis agent was dropwise added to $Ti(OBu)_4$ (Aldrich) and CTMA-Cl (Aldrich) mixture with precision control of reaction media pH value under vigorous stirring for 6 hours at 60–65°C with the next sol ageing for 4 days at room temperature. Five titania samples were obtained at pH values of 1.0, 1.2, 1.4, 1.6 and 1.8 and were marked as M1–M5, respectively. Obtained colloidal solution was separated by centrifugation, washed with distilled water and dried at 85°C; additional washing with absolute ethanol was used for template (surfactant) extraction.

The structure of materials was investigated by XRD (DRON-4-07 diffractometer, CuK_α radiation, Bragg–Brentano geometry, NiK_β-filter). Low-temperature nitrogen adsorption method was used for morphology analysis (Quantachrome Autosorb Nova 2200e porosimeter; adsorption–desorption isotherms were measured at 77 K). The samples surface area was calculated by the Brunauer–Emmett–Teller (BET) method.

3. RESULTS AND DISCUSSION

It is known that the degree of hydrolysis is a function of reaction media pH, and it determines the type of primary monomers formed during the hydrolysis of titanium salts [1]. The reaction

$Ti(OC_4H_9)_4 + nH_2O \rightarrow Ti(OH)_n(OC_4H_9)_{4-n} + nC_4H_9OH$ occurs during the hydrolysis of titanium butoxide. $[Ti(OH_2)_6]^{4+}$ monomers, where Ti^{4+} ions are octahedrally co-ordinated, are formed at the final stage of hydrolysis. The protolysis is happened as $[Ti(OH_2)_6]^{4+} + hH_2O \leftrightarrow$ $\leftrightarrow [Ti(OH)_h(OH_2)_{6-h}]^{(4-h)+} + yH_3O^+$ where h is a hydrolysis ratio. In $[Ti(OH)_h(OH_2)_{6-h}]^{(4-h)+}$, the OH groups are located in the equatorial planes of the octahedron, and the H_2O molecules primarily occupy the vertex position [2]. Applying the partial charge theory [3], the hydrolysis ratio h was calculated from the pH (Fig. 1). It was determined that, for investigated pH range, $[Ti(OH)_2(OH_2)_4]^{2+}$ species are the most probable hydrolysis products when the pH increasing leads to increasing the possibility of $Ti(OH)_3(OH_2)_3]^+$-complexes' formation. The pH values less 2 are the preconditions of rutile phase nucleation because of primary monomers' condensation by joint edges in equatorial planes of octahedra [4]. The increasing of hydrolysis ratio leads to the anatase or brookite phases' formation because of the merger of co-ordination octahedra by lateral planes of faces. At the same time, both the chelating and bridging bidentate complexes' formation between sulphate anions and octahedrally co-ordinated $[Ti(OH)_2(OH_2)_4]^{2+}$ monomers stimulates screw polymer chains formation and the nucleation of TiO_2-anatase phase.

Hexadecyltrimethylammonium bromide (CTAB) molecules in aqueous solution lose Br^- and, when the surfactant concentration exceed threshold of $0.9 \cdot 10^{-3}$ mole$\cdot$L^{-1} form spherical micelles [5]. In our experiment, the concentration of CTAB was about $12 \cdot 10^{-3}$ mole$\cdot$L^{-1}, so, at this condition, $CTMA^+$ ions form a hexagonal array of cylindrical micellae with hydrophobic alkyl inside and charged hydrophilic groups on the outer side. The titania nucleation in this array of tubular channels with the further template extraction leads

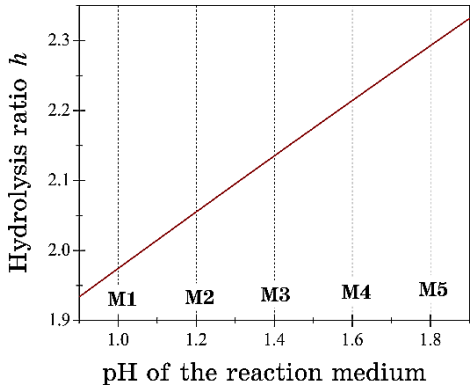

Fig. 1. Dependence of the hydrolysis ratio h of $[Ti(OH)_h(OH_2)_{6-h}]^{(4-h)+}$ monomers on the pH of the reaction medium.

to mesoporous materials obtaining.

All materials obtained by initial xerogels' drying at 80°C and ethanol extraction are amorphous (XRD data; see Fig. 2, *a*) states with anatase structural motives and crystallized to nanostructured anatase after annealing at 500°C. It was determined (low-angle x-ray scattering data) that the titania samples have mesoporous morphology (Fig. 2, *b*).

The Bragg spacing value for (100) reflex of ordered structure is of 2.5 nm, and hexagonal lattice constant is of 2.9 nm. Specific surface areas (low-temperature nitrogen adsorption data, BET model) non-linearly vary depending on the pH in a range of 88–348 m^2/g with the maximum for M3 sample obtained at pH = 1.4 (Fig.

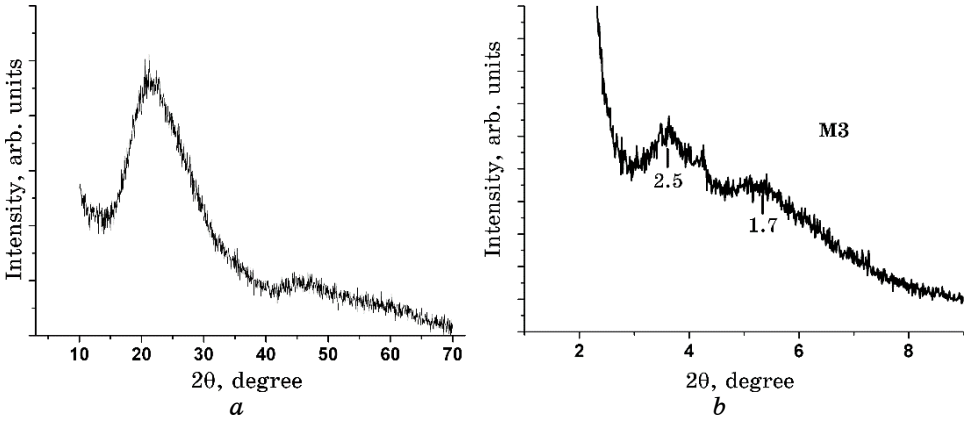

Fig. 2. Low-angle XRD pattern for M3 sample at annealing temperatures of 80°C (*a*) and 500°C (*b*).

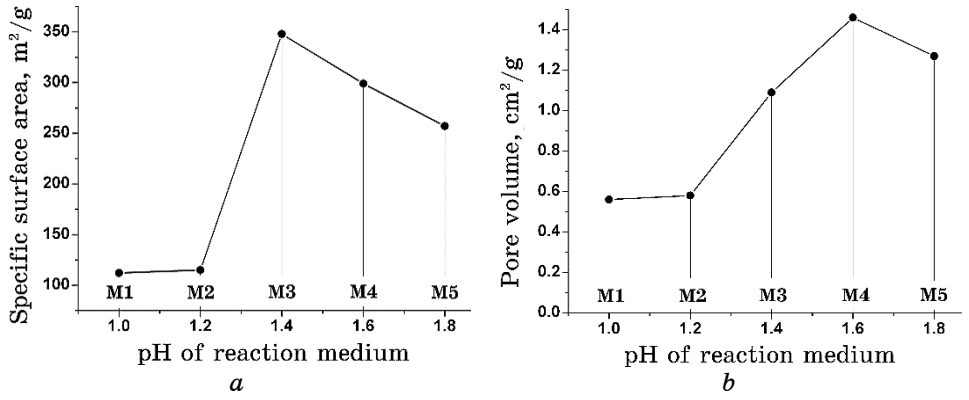

Fig. 3. The specific surface area (*a*) and total mesopore volume (*b*) of titania samples obtained at different pH of reaction medium.

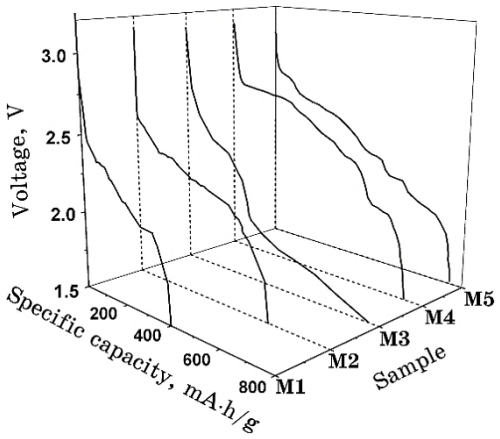

Fig. 4. The discharge curves of the model lithium power sources with the cathode on the base of mesoporous titania samples.

3, *a*). Total specific volume of mesopores (equivalent model of cylindrical pores) changes in the range of 0.56–1.68 cm^3/g (Fig. 3, *b*).

The obtained titania samples were used as a base of the electrode materials for the model lithium power sources. Electrode composition consist of titania (90 mass.%), acetylene black (8 mass.%) and PVDF (2 mass.%). Polarizing and comparison electrodes were made from lithium foil; 1M $LiBF_4$ in γ-butyrolactone was used as the electrolyte. The discharges were carried out in galvanostatic conditions at current density of C/10. Character of the discharge curve is the result of the different processes domination at different stages of discharge: intercalation, formation of double electric surface layer, change of material phase composition (Fig. 4).

The obtained values of specific power density vary in a range of 870–1750 W/kg. Specific capacity and power density increase with the pore volume and specific surface area enlarging (Fig. 5, *a*, *b*). The kinetics of the discharge process was investigated by means of the impedance spectroscopy. The presence of the only one kinetic process during discharge was determined. Diffusion coefficients, calculated accordingly to [6], decline exponentially with the increasing of intercalation degree in a range of $1 \cdot 10^{-8}$–$2 \cdot 10^{-11}$ cm^2/s.

4. CONCLUSIONS

Mesoporous titania with ordered hexagonal structure has been prepared using CTMA-Cl-template-assisted sol–gel route. The specific surface areas of titania samples change in a range of 88–348 m^2/g depending on the pH of reaction medium during hydrolysis. The

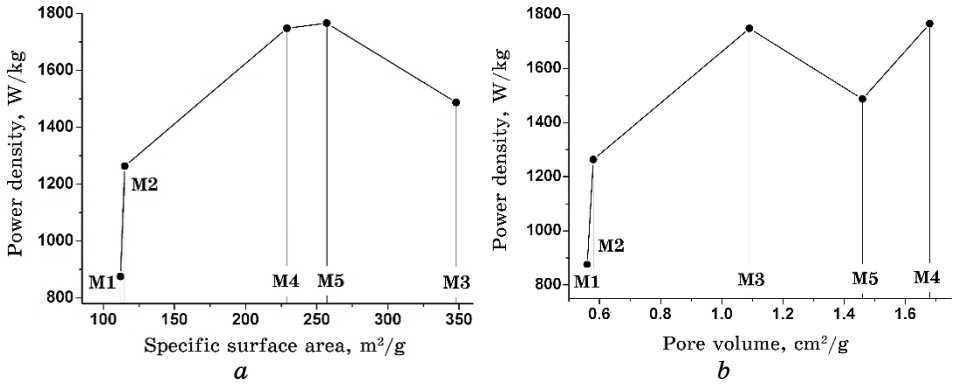

Fig. 5. Power density of the Li^+-ions' electrochemical intercalation for electrode materials on the base of mesoporous titania as a function of specific surface area (*a*) and total mesopore volume (*b*).

specific power densities of Li^+-ions' intercalation vary in a range of 870–1750 W/kg for titania samples with different total mesopore volumes and specific surface areas.

REFERENCES

1. V. O. Kotsyubynsky, I. F. Myronyuk, L. I. Myronyuk, V. L. Chelyadyn, M. H. Mizilevska, A. B. Hrubiak, O. K. Tadeush, and F. M. Nizamutdinov, *Mater. Sci. Forum*, **47**, Nos. 2–3: 288 (2016); https://doi.org/10.1002/mawe.201600491
2. S. G. Kumar and K. K. Rao, *Nanoscale*, **6**, No. 20: 11574 (2014); https://doi.org/10.1039/C4NR01657B
3. M. Henry, J. P. Jolivet, and J. Livage, *Structure and Bonding. Vol. 77. Chemistry, Spectroscopy and Applications of Sol–Gel Glasses* (Eds. R. Reisfeld and C. K. JJørgensen) (Berlin–Heidelberg: Springer: 1992); https://doi.org/10.1007/BFb0036968
4. V. Kotsyubynsky, I. Myronyuk, V. Chelyadyn, A. Hrubiak, V. Moklyak, and S. Fedorchenko, *J. Nano Research*, **50**: 32 (2017); DOI: 10.4028/www.scientific.net/JNanoR.50.32
5. B. Naskar, A. Dan, S. Ghosh, V. K. Aswal, and S. P. Moulik, *J. Mol. Liq.*, **170**: 1 (2012); https://doi.org/10.1016/j.molliq.2012.03.020
6. S. Liu, J. Zhang, K. Huang, and J. Yu, *J. Braz. Chem. Soc.*, **19**: 1078 (2008); https://doi.org/10.1590/S0103-50532008000600005